An *ab Initio* Hartree−Fock Study of the Cubic and Tetragonal Phases of Bulk Tungsten Trioxide

Furio Corà,*,† Atul Patel,† Nicholas M. Harrison,‡ Roberto Dovesi,§ and C. Richard A. Catlow†

Contribution from the Davy Faraday Research Laboratory, The Royal Institution of Great Britain, 21 Albemarle Street, London W1X 4BS, U.K., CLRC Daresbury Laboratory, Daresbury, Warrington WA4 4AD, U.K., and Gruppo di Chimica Teorica, Università di Torino, Via Giuria 5, 10125 Torino, Italy

Received May 6, 1996. Revised Manuscript Received July 15, 1996[⊗]

Abstract: The structural and electronic properties of bulk cubic and tetragonal tungsten trioxide are investigated using a periodic boundary condition *ab initio* Hartree−Fock method; *a posteriori* density functional corrections are used to estimate the effect of electron correlation on the energy. The forces involved in the bonding between metal and oxygen are examined to shed light on the crystal chemistry of the compound. While the cubic phase is highly ionic, the symmetry distortion leading to the tetragonal phase causes an increase in covalence between tungsten and its nearest oxygen. The observed instability of cubic WO_3 is explained by its higher energy (0.80 eV per formula unit) with respect to the tetragonal phase. We attribute this energy difference to the increased covalence observed in the latter phase. The calculated structural parameters for tetragonal WO_3 agree with available experimental data. A layered structure emerges from our calculations for tetragonal WO_3; when the effect of applying pressure is examined, only the interlayer spacing is appreciably modified. This softer degree of freedom results in a lower value of the bulk modulus when compared to that of the cubic phase. In the range of experimentally obtainable pressures, the order of stability of the two phases cannot be reversed, and the cubic structure remains unstable with respect to the tetragonal structure.

I. Introduction

Corner-sharing octahedral networks are common in the structural chemistry of the binary and ternary transition metal oxides and halides.[1] The most widespread structure type is that adopted by the naturally occurring mineral perovskite $CaTiO_3$. The well-known structure is illustrated in Figure 1, together with projections in two perpendicular crystallographic planes. In the ternary compounds, the larger cation occupies the 12-fold coordinated site of the oxygen sublattice (labeled A in Figure 1), while the octahedral network is constructed from corner-sharing of the BX_6 octahedra of the smaller, B-type cation. Binary compounds based on octahedral networks are also known. Some, such as ReO_3[2] and MoF_3,[3] are found in the ideal cubic structure; in others like β-MoO_3[4,5] and WO_3, oxygen octahedra are deformed and tilted, and the metal ion lies off-center. Such distortions are a major feature of the structural chemistry of both binary and ternary compounds based on octahedral networks. An earlier discussion of the problem can be found in ref 6, where group theory arguments, coupled with model extended Hückel calculations, are employed to analyze the driving force for the distortions. In this paper we employ accurate, periodic boundary condition, *ab initio* calculations to examine the case of tungsten trioxide: structure deformations of the type described above lead to phases that range, as a function of temperature, from triclinic to tetragonal,[7−12] while the highest symmetry cubic structure has never been observed experimentally. Our study aims at providing a global insight into the structure and bonding in this class of compounds.

Interest in the specific case of tungsten oxide is also stimulated by its catalytic activity toward different reactions,[13−15] from the ability to incorporate cations and form insertion compounds (the tungsten bronzes),[16] and from its electronic behavior;[17] it shows in fact ferroelectric, electrochromic, and semiconducting properties.

Despite these applications, and the more general importance of the structural type, detailed structural data on WO_3, both experimental and theoretical, are still lacking. Experimental difficulties arise from the tendency of the solid to form substoichiometric shear phases[18] and twinned crystals;[10] theoretical problems are due to the presence of the heavy atom and to the low symmetry of the existing structures. This study aims to fill this gap, and answer fundamental questions concerning the crystal chemistry of the compound. More specifically we propose to investigate the forces involved in the bonding

† The Royal Institution of Great Britain.
‡ CLRC Daresbury Laboratory.
§ Universitá di Torino.
⊗ Abstract published in *Advance ACS Abstracts,* November 15, 1996.

(1) Wyckoff, R. W. G. *Crystal Structures*, 2nd ed.; Interscience: New York, 1965.
(2) Biltz, W.; Lehrer, G. A.; Meisel, K. *Z. Anorg. Allg. Chem.* **1932**, *207*, 113.
(3) La Valle, D. E.; Steele, R. M.; Wilkinson, M. K.; Yakel, H. L., Jr. *J. Am. Chem. Soc.* **1968**, *82*, 2433.
(4) McCarron, E. M., III. *J. Chem. Soc., Chem. Commun.* **1986**, 336.
(5) Parise, J. B.; McCarron, E. M., III; Von Dreele, R.; Goldstone, J. A. *J. Solid State Commun.* **1991**, *93*, 193.
(6) Wheeler, R. A.; Whangbo, M.-H.; Hughbanks, T.; Hoffmann, R.; Burdett, J. K.; Albright, T. A. *J. Am. Chem. Soc.* **1986**, *108*, 2222.
(7) Kehl, W. L.; Hay, R. G.; Wahl, D. *J. Appl. Phys.* **1952**, *23*, 212.
(8) Wyart, J.; Foex, M. *C. R. Acad. Sci.* **1951**, *233*, 2459.
(9) Salje, E. *Acta Crystallogr., B* **1977**, *33*, 574.
(10) Loopstra, B. O.; Boldrini, P. *Acta Crystallogr.* **1966**, *21*, 158.
(11) Salje, E.; Viswanathan, K. *Acta Crystallogr., B* **1975**, *31*, 356.
(12) Diehl, R.; Brandt, G.; Salje, E. *Acta Crystallogr., B* **1978**, *34*, 1105.
(13) Ai, M. *J. Catal.* **1977**, *49*, 305.
(14) Yamaguchi, T.; Tanaka, Y.; Tanabe, K. *J. Catal.* **1980**, *65*, 442.
(15) Lietti, L.; Svachula, J.; Forzatti, P.; Busca, G.; Ramis, G.; Bregani, F. *Catal. Today* **1993**, *17*, 131.
(16) Sienko, M. J. In *Non-Stoichiometric Compounds*; Gould, R. F., Ed.; Advances in Chemistry Series; ACS: Washington, DC, 1963. Dickens, P. G.; Whittingham, M. S. Q. *Rev. Chem. Soc.* **1968**, *22*, 30.
(17) Salje, E. *J. Appl. Crystallogr.* **1974**, *7*, 615.
(18) Sundberg, M.; Tilley, R. J. D. *J. Solid State Chem.* **1974**, *11*, 150.

S0002-7863(96)01514-4 CCC: $12.00

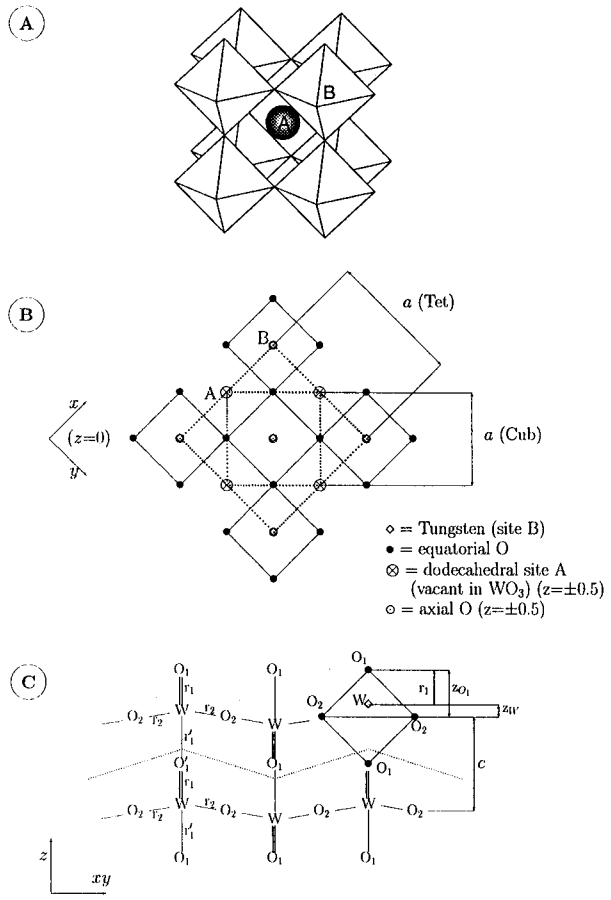

Figure 1. (A) Geometry of the perovskite structure. (B) Projection in the *xy* plane, showing the corner-sharing connection between oxygen octahedra; the interstitial sites A and B of the oxygen sublattice are marked, as described in the text. The edges of the unit cell of the cubic and tetragonal phases of WO_3 are marked with a dotted line. (C) Projection along the crystallographic *c* axis of the tetragonal phase of WO_3, to illustrate the geometric parameters used. The dotted line identifies the layered structure of the solid, and shows the interlayer separation.

between metal and oxygen, and to understand why the parent cubic structure is unstable. Notwithstanding the recent advance in computer simulation techniques and hardware, the computational requirements for the *ab initio* description of solid materials are still very demanding; attention in this study has therefore been limited to the highest symmetry, cubic and tetragonal phases of WO_3.

This paper is organized as follows: In section II the computational details are given, and we describe the procedure adopted to optimize the tungsten basis set. Section III contains results for the two phases examined. An explanation is given as to why the cubic phase is unstable. The effect of pressure on the structures is examined in section IV. Finally, section V summarizes the major findings of the present study.

II. Basis Set and Computational Details

The model we have adopted to study the bulk material is based on periodic boundary conditions at the Hartree−Fock (HF) level of approximation, as implemented in the code CRYSTAL.[19,20] The electronic distribution of the solid is described in terms of crystalline orbitals; these are obtained as linear combinations of localized functions, or atomic orbitals (AOs), associated with lattice sites.

Table 1. Optimized Tungsten Basis Sets and Those Used in This Work

	exponent		coefficient	
shell type	optimized	used	s	p or d
sp	0.488	0.600	1.000	1.000
sp	0.157	0.200	1.000	1.000
d	1.223			0.097
	0.963			0.241
	0.377			0.530
d	0.260			1.000

Prior to the present investigation, no *ab initio* study involving ionic tungsten in the solid state has been performed with this technique, hence making the first task that of optimizing a suitable basis set. Because of the presence of the heavy tungsten atoms, it is convenient to avoid core electrons, and adopt the well-assessed effective core pseudopotential (ECP) techniques.[21,22] The large-core ECP derived by Hay and Wadt[21] has been chosen for tungsten; this leaves only the 5d and 6sp valence electrons to be explicitly described on the metal site. A split-valence basis set has been adopted, composed of two independent, single Gaussian sp shells, and a 3-1G contraction for d electrons. This basis has been variationally optimized in the cubic phase; although this phase does not exist experimentally, the major characteristics of the crystal field are reproduced, and the exploitation of the higher symmetry makes the optimization less computationally demanding. We have not used the standard procedure of optimizing the basis set for the isolated ion, because of the initial assumptions about the ECP: the isolated W^{6+} ion described with a large core ECP, in fact, has no valence electrons. When the tungsten ion occupies its lattice position, its basis functions contribute to the overall description of the solid; it is this contribution that has been optimized using a variational procedure. The geometry of the cubic phase used during the basis set optimization has been chosen in such a way that the volume per formula unit is the same as the experimental value for the tetragonal structure.[7] The resulting lattice parameter for the cubic cell, *a*, is 3.7787 Å. The sp functions optimized in the above procedure correspond to diffuse orbitals that extend over the neighboring lattice sites. In the periodic model that we have adopted, this diffuseness can lead to pseudolinear dependence problems in the solution and instabilities in the SCF convergence.[19] In these calculations we have therefore used less diffuse functions, as reported in Table 1.

Oxygen ions are described with an all-electron 8-51G set, already used in highly ionic compounds.[23−25] Basis sets of this quality have proved adequate to describe most crystalline materials;[20] the presence of unoccupied AOs on both the anionic and cationic sites gives flexibility to the basis, and allows the polarizability of both species in their crystalline environment and the back-donation of electrons from the oxygens to the metal to be taken into account.

In the CRYSTAL code, the accuracy in the evaluation of the Coulomb and exchange series is controlled by a set of tolerances (see ref 20 for details); in the present case very high values (8, 7, 8, 8, 16) have been used, which ensure low numerical noise in the geometry optimization procedure. Reciprocal space integrals are performed as a weighted sum at a discrete set of *k*-points. The *k*-points employed sample uniformly the first Brillouin zone, and include all high symmetry positions of the reciprocal lattice; weights are attributed according to the Pack−Monkhorst scheme.[26] The number of *k*-points is chosen in such a way that the results of the numerical integration are well converged; in the results reported in the following sections, 75 *k*-points were used to sample the first Brillouin zone of tetragonal WO_3.

(19) Pisani, C.; Dovesi, R.; Roetti, C. HF ab-initio treatment of crystalline systems. *Lecture Notes in Chemistry*; Springer-Verlag: Heidelberg, 1988; Vol. 48.
(20) Dovesi, R.; Saunders, V. R.; Roetti, C. *CRYSTAL92 User's manual*; Gruppo di Chimica Teorica, University of Turin, Turin, Italy, 1992.
(21) Hay, P. J.; Wadt, W. R. *J. Chem. Phys.* **1985**, *82*, 270, 284, 299.
(22) Durand, P. H.; Barthelat, J. C. *Theor. Chim. Acta* **1975**, *38*, 283.
(23) Causà, M.; Dovesi, R.; Pisani, C.; Roetti, C. *Phys. Rev. B* **1986**, *33*, 1308.
(24) Nada, R.; Catlow, C. R. A.; Dovesi, R.; Pisani, C. *Phys. Chem. Miner.* **1990**, *17*, 353.
(25) D'arco, P.; Sandrone, G.; Dovesi, R.; Orlando, R.; Saunders, V. R. *Phys. Chem. Miner.* **1993**, *20*, 407.
(26) Monkhorst, H. J.; Pack, J. D. *Phys. Rev. B* **1976**, *13*, 5188.

Table 2. Cost of the Computations for the Two Phases Examined[a]

	cubic phase	tetragonal phase		cubic phase	tetragonal phase
space group	*Pm*3*m*	*P*4/*nmm*	time/integrals	430	1362
N atoms/cell	4	8	time/SCF	180	1536
N AOs/cell	45	90	N_{red}	85975	171942
storage	1.86	14.73			

[a] Storage refers to the disk space required to store integrals, in units of M_{words}; N_{red} is the number of elements of the Hamiltonian matrix explicitely calculated. Times correspond to the total cpu time, in seconds, to perform a single point parallel calculation on a cluster of 4 HP-730 workstations; convergence to 10^{-6} hartree is reached in both cases in 18−19 SCF cycles.

Calculations have been performed on a cluster of four HP-730 workstations. Table 2 reports the cost of the computations, in terms of cpu time and storage requirements, for the two phases examined.

Finally, in the following sections, HF results have been corrected in order to take into account electron correlation; its contribution to the energy has been evaluated *a posteriori*, with a density functional, according to the scheme proposed by Perdew et al.[27,28] No correction has instead been attempted for the HF wave function.

III. Results and Discussion

The results reported in this section refer to the ground state electronic structure and related properties. Different aspects have been examined, and are discussed separately in the following sections.

a. Geometric Parameters. Let us start by examining the geometry of the cubic and tetragonal structures. In the hypothetical cubic phase, also referred to as the ReO_3 structure,[2] the metal atom is surrounded by a regular octahedron of six nearest oxygens; the unit cell contains a single formula unit WO_3. All internal coordinates are unambiguously determined by symmetry constraints; this leaves a single degree of freedom, the lattice parameter *a*. The tetragonal unit cell contains two formula units; the structure is schematically shown in Figure 1C. Two sets of inequivalent oxygen ions are present, which we can refer to as axial oxygens (O_1 and O_1' in Figure 1B), disposed along the crystallographic *c* axis, and equatorial oxygens (O_2). The tetragonal phase has four independent degrees of freedom: the lattice parameters *a* and *c*, and the internal coordinates of the tungsten and of the axial oxygen ions (z_W and z_{O_1}, respectively). Starting from the cubic geometry, the symmetry reduction leading to the tetragonal structure can be obtained in two independent ways: by changing the *a*/*c* ratio, or by displacing the tungsten ion off-center along the *z* direction in its coordination polyhedron.

The four geometric parameters can be re-expressed in a different way, with a more direct physical meaning:

$$\begin{cases} V = a^2 c \\ d = a/c \\ r_1 = c(z_{O_1} - z_W) \\ z_W \end{cases} \quad (1)$$

In this new notation *V* is the unit cell volume. The parameter *d* represents the tetragonal deformation of the oxygen polyhedra: in the ideal cubic structure $d = \sqrt{2} = 1.4142$; the more *d* differs from this value, the more the octahedron of oxygens is distorted around the metal center. r_1 is the distance between tungsten and its nearest oxygen. z_W the displacement (in units of *c*) of the tungsten ion from the center of its coordination polyhedron. z_W is again a measure of the deviation from the cubic structure, where it assumes the value $z_W = 0$.

b. Structure Optimization, Bond Structure, and Electronic Distribution. The two phases examined have been completely optimized, both at the HF level and with correlation. The resulting geometries are reported in Table 3. For subsequent reference we also report in the last column of Table 3 the value of the bulk modulus, as discussed in section IV.

The nature of the bonding in the cubic phase, which emerges from the calculations, is predominantly ionic. In the optimized HF geometry the Mulliken population analysis attributes a net charge of +4.086 |e| to the tungsten ion, and −1.362 |e| to each of the oxygens. The bond population between tungsten and its six nearest neighbors is $q_b = -0.027$ |e|, showing a slight antibonding character, and indicating that no major covalent effect is present in the solid. The overall value of q_b arises from the balance between a small bonding contribution involving the metal d AOs of both σ ($q_b^{d,\sigma} = 0.13$ |e|) and π symmetry ($q_b^{d,\pi} = 0.08$ |e|) along the W−O direction, and an antibonding combination involving the metal sp AOs. The total occupancy of d levels on tungsten is appreciable (2.57 |e|); a population of −0.65 |e| is attributed to the tungsten sp AOs. This negative value, due to antibonding combinations with the occupied oxygen AOs, has already been noted in a previous study on ZrO_2;[30] the large value is related to the diffuse character of the tungsten sp AOs, which have a large overlap with the oxygen basis functions.

In terms of a localized representation of the bonding, as employed in coordination chemistry, we can idealize the interaction between metal and oxygen in cubic WO_3 as between classic ions, W^{6+} and O^{2-}, with a considerable back-donation of electrons from the filled oxygen sp AOs to the vacant metal d AOs. The back-donation effect involves, to a comparable extent, orbitals of both σ and π symmetry along the W−O directions.

In the optimization of the tetragonal structure we started from the equilibrium cubic geometry. In this procedure we aimed at exploiting the possibility that is offered by computational studies to focus on single chemicophysical effects, by examining separately single degrees of freedom of the system. During the optimization, we have first kept fixed the volume per formula unit to its HF value in the cubic phase (V_o) and explored separately the two previously mentioned distortions, varying *d* and z_W, respectively. The energy changes associated with these two parameters are shown in Figure 2 (A and B). When *d* is changed, but the tungsten ion is maintained in-center in its octahedron ($z_W = 0$, Figure 2A), the electronic distribution is only slightly modified, and the structure remains ionic. The energy minimum corresponds to the cubic value $\sqrt{2}$. This result allows us to rule out a first-order Jahn−Teller distortion[29] as the major cause for the stabilization of the tetragonal phase with respect to the cubic phase. It is also consistent with a classical description of tungsten as of a 6+, $d^{(0)}$ ion; there is in fact no d electron associated with the metal center to provide the driving force for the Jahn−Teller distortion. The driving force for the symmetry lowering in WO_3 cannot therefore be attributed to a change involving tungsten ions alone, and must involve the oxygens.

Only when z_W is changed and tungsten displaced off-center toward one of its nearest neighbors, do we observe a stabilization of the tetragonal structure (Figure 2B). Ferroelectric and antiferroelectric displacements of tungsten are both energetically

(27) Perdew, J. P. In *Electronic Structure of Solids*; Ziesche, P., Eschrig, H., Eds.; Akademic Verlag: Berlin, 1991.
(28) Perdew, J. P.; Chevary, J. A.; Vosko, S. H.; Jackson, K. A.; Pederson, M. R.; Singh, D. J.; Fiolhais, C. *Phys. Rev. B* **1992**, *46*, 6671.
(29) Kugel, K. I.; Khomskii, D. I. *Sov. Phys. Usp.* **1982**, *25*, 231.
(30) Orlando, R.; Pisani, C.; Roetti, C.; Stefanovich, E. *Phys. Rev. B* **1992**, *45*, 592.

Table 3. Calculated and Experimental Structures for WO_3 and Structural Data at Equilibrium[a]

phase	param	HF	HF + corr	experiment		
cubic	V	53.37	51.48		ne	
	d	1.414	1.414		ne	
	r	1.882	1.860		ne	
	z_W	0.000	0.000		ne	
	B	257	281		ne	
	E_o	−232.0549	−233.1844			
tetragonal	V	55.50	52.67	53.95	54.48	51.95
	d	1.318	1.319	1.341	1.345	1.345
	r	1.629	1.636	na	na	na
	z_W	0.085	0.089	0.06	0.06	na
	B	137	174	na	na	na
	E_o	−464.1682	−466.4171			
				ref 7 T = 770 °C	ref 7 T = 950 °C	ref 11 T = 740 °C

[a] Symbols have the meaning defined in the text and shown in Figure 1. For the experimental values, ne means that the corresponding phase does not exist, while na refers to the fact that the corresponding value has not been reported in the experimental work. The rows indicated with B report the calculated values for the bulk modulus, in GPa (1 GPa = 10^4 atm); E_o is the energy per unit cell of the fully optimized structures, in hartrees.

favored, and cause a shortening of the equilibrium bond length between tungsten and the nearest oxygen from 1.882 to 1.656 and 1.626 Å, respectively. The energy gain associated with the W movement along z is different in the two cases: 0.58 eV per formula unit in the antiferroelectric deformation, in which the metal ions displace along alternate directions, and only 0.28 eV per formula unit in the ferroelectric deformation, in which all metal ions displace uniformly with respect to the oxygen sublattice. The stability of the distorted structure was predicted in ref 6 by examining the changes in the one-electron energy levels during the tungsten displacement. No comparison was however effected in ref 6 for ferro- and antiferroelectric displacements. In our model of the solid, all interactions are correctly described: both short-range (in particular between nearest neighbors and next nearest neighbors) and long-range ones, due to the crystal field. While the former are comparable in ferro- and antiferroelectric deformations (which is confirmed by the similarities in the W−O equilibrium distance), the behavior is differentiated by long-range effects. Comparing the energy gains, we see that short- and long-range interactions play a comparable role in determining the solid state chemistry of WO_3. The overall behavior is therefore due to a subtle balance of different contributions; and limiting the analysis to only one can provide misleading information.

The relative energy of the ferro- and antiferroelectric structures is in agreement with the experimentally observed structure of tetragonal WO_3, and in the remainder of this paper we make reference only to the antiferroelectric structure. The energy associated with the W movement along z is consistent with a change in the chemical bonding in the solid. As the tungsten ion is displaced, along with the energy gain we observe an accumulation of electrons in the region between the metal and its nearest oxygen, that is, an *increase of covalence* in this W−O bond. We examine this effect more extensively later.

In the next step of the optimization procedure, we have performed a full geometric relaxation of the tetragonal structure around the displaced tungsten ion, but still maintained the volume fixed at its equilibrium value in cubic WO_3, V_o. Once tungsten is displaced off-center, the relaxation of the oxygen octahedra contributes to stabilizing the structure. The parameter d representing the tetragonal distortion is now 1.319, significantly different from the cubic value $\sqrt{2}$. The deformation of the oxygen sublattice corresponds to a compression in the equatorial plane (at the HF level, the lattice parameter a changes from 5.324 to 5.196 Å) and to an elongation along the z direction (the lattice parameter c increases from 3.765 to 3.939 Å). Despite the pronounced rearrangement of the oxygens around the metal, the value of the shortest W−O distance, r_1, is only marginally affected, and changes from 1.626 Å obtained in the previous step to 1.629 Å. The equilibrium value for r_1 is therefore a *local* property of the short, strong W−O bond, rather than a collective property of the solid, a result which confirms the previous analysis of the covalent character of the interaction.

Finally, the optimization procedure has been repeated for different volumes of the unit cell, to obtain the absolute minimum. The energy variation as a function of V is shown in Figure 2C, while Table 4 reports the dependence on V of the equilibrium geometry parameters. Again we note that, on changing V, the value of r_1 changes little, by less than 0.01 Å, while d and especially z_W vary more appreciably. On changing the volume V, the new equilibrium geometry is thus obtained shifting rigidly the bonded W−O couple and compressing the equatorial oxygens. This behavior highlights the existence in the solid of a "rigid" feature, represented by the covalent bond, and of a softer one, corresponding to deformations of the polyhedron of ionically bonded oxygens. The covalently-bound W−O couple behaves as a single unit, and we can therefore refer to it as a *tungstyl* group. The difference in energy between the two fully optimized phases is 0.80 eV per formula unit at the HF level (0.66 eV with correlation corrections), and is largely dominated by the increased covalence between tungsten and the nearest oxygen. The strength of the covalent bond formed is sufficient to explain the instability of the cubic structure.

The transformation from the cubic to the tetragonal phase corresponds to an increase of the volume per formula unit; this increase is slightly larger for the HF than for the correlated results (3.99% and 2.31%, respectively). Comparing calculated and experimental geometries, we find finally that the calculated deformation is slightly overestimated (d = 1.32 vs 1.34; z_W = 0.09 vs 0.06). We should note, however, that the calculated values are obtained at a temperature of 0 K, while the experimental ones correspond to a much higher temperature ($T \simeq$ 1000 K). We must also underline the high error bars associated with the experimental values; in particular the internal coordinates of the axial oxygen ions[7] have an uncertainty of $0.06c \simeq 0.24$ Å in the z direction.

The HF equilibrium geometry and population analysis around the metal center are reported in Table 5. In the cubic phase, the six nearest neighbor oxygens are symmetrically equivalent; in the tetragonal phase they are resolved into three different groups. While the distance of the four equatorial oxygens from

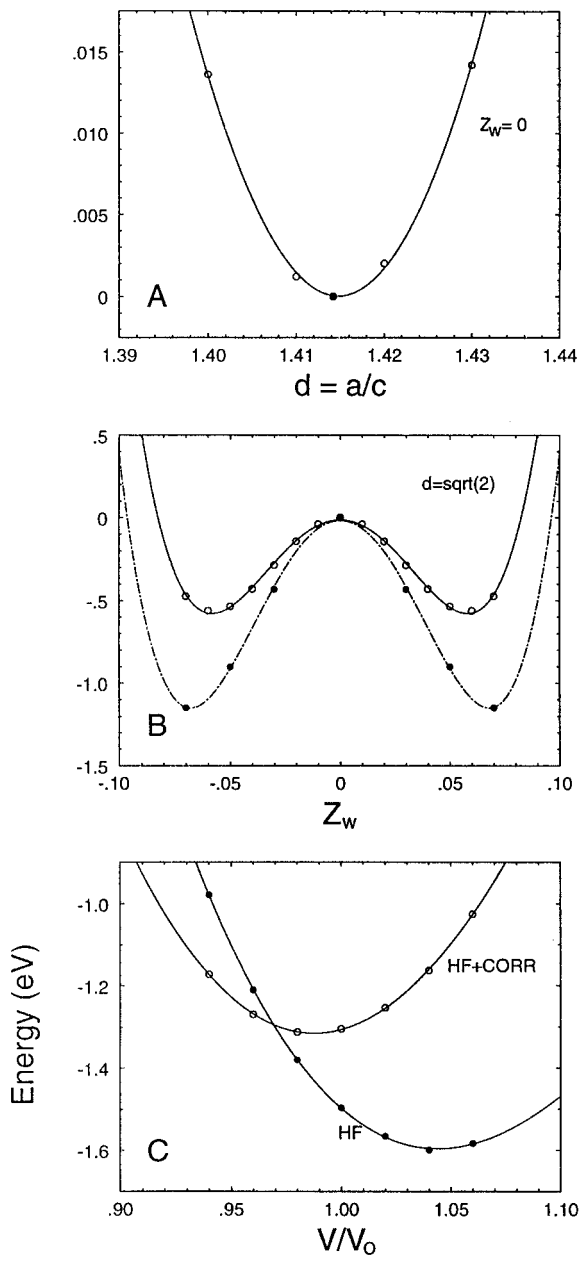

Figure 2. Dependence of the total energy of tetragonal WO_3 (eV) on different geometric parameters. (A) Tetragonal deformation (d) of the oxygen octahedra, with tungsten in-center. (B) Ferro- (open circles) and antiferroelectric (filled circles) displacement of tungsten. The oxygen sublattice is kept fixed in the cubic phase. (C) Volume per formula unit for tetragonal WO_3. Open circles refer to the HF energy, filled circles to the correlation-corrected data. V_o is the HF equilibrium volume for cubic WO_3. The zero of energy has been chosen as coincident with the equilibrium energy in the cubic phase. For each volume V the structure has been fully optimized. Note the different energy scale of (A) with respect to (B) and (C).

the central tungsten remains almost unchanged at 1.89 Å, the axial oxygens O_1 and O_1' are now at considerably different distances. This anisotropy is reflected in the Mulliken charges: again the value for equatorial oxygens is very similar to that in cubic WO_3 (-1.410 vs -1.362 |e|), while in the axial oxygens we observe a substantial decrease to -0.973 |e|, compensated by a simultaneous decrease of the positive charge on tungsten. The trend is consistent with the increase in covalence in the interaction between the latter two species.

Figure 3 shows the difference electron density maps for the optimized HF geometries. The maps are obtained by subtracting the density of isolated W^{6+} and O^{2-} ions from the total density

Table 4. Equilibrium Configuration and Bond Distances of Tetragonal WO_3 as a Function of the Volume per Formula Unit[a]

	HF			HF + Correlation				
V/V_o	d	z_W	r_1	d	z_W	r_1	r_2	r_1'
0.96	1.320	0.095	1.631	1.320	0.092	1.636	1.850	2.253
0.98	1.320	0.092	1.630	1.319	0.089	1.636	1.860	2.282
1.00	1.319	0.090	1.629	1.319	0.087	1.635	1.871	2.309
1.02	1.319	0.087	1.628	1.318	0.084	1.635	1.881	2.337
1.04	1.318	0.085	1.629	1.317	0.081	1.634	1.891	2.366
1.06	1.316	0.083	1.628	1.315	0.079	1.633	1.900	2.396
						-0.18^b	$+2.70^b$	$+6.37^b$

[a] V_o is the HF equilibrium volume per formula unit of cubic WO_3; symbols for distances are shown in Figure 1B. [b] Percent change.

Table 5. Bond Structure and Charges around the Metal Center at the HF Equilibrium Geometry for Cubic and Tetragonal WO_3[a]

atom	multiplicity	net charge	bond distance	bond population
		Cubic Phase		
W	1	+4.086		
O	6	−1.362	1.883	−0.027
		Tetragonal Phase		
W	1	+3.793		
O_1	1	−0.973	1.629	0.214
O_2	4	−1.410	1.895	−0.008
O_1'	1	−0.973	2.366	−0.004
⟨O⟩	6	−1.264	1.929	0.030

[a] Bond distances are reported in angstroms and charges in units of |e|. The row ⟨O⟩ reports the averaged data for the six nearest neighbor oxygens in the tetragonal structure.

of the solid. The former are spherical species; in this way all features of the electronic distribution in the solid are highlighted. The maps are drawn in the plane containing the metal (at the center) and four of its six nearest neighbor oxygens: the two axial O_1 and O_1' and two equatorial O_2 (the same cut of the solid displayed in Figure 1B) so that all the features of the bonding are shown.

The electronic distribution around oxygen ions is considerably distorted by the presence of the two nearest tungsten ions. In a multipolar expansion of the charge distribution, this polarization effect results in the presence of poles of higher order; in the cubic phase the dipole is absent because of symmetry constraints, but a strong quadrupole moment on the oxygen ions is clearly visible in the map of Figure 3. In the tetragonal phase (right plot), the map shows the anisotropy in the different metal−oxygen bonds. The distortion in the charge distribution is higher than in the cubic phase.

The increase of electronic charge in the region between tungsten and the nearest oxygen, O_1, associated with the increased covalence in tetragonal WO_3, is quite evident. This effect can be given a more quantitative description by referring again to a Mulliken population analysis. The bond population, q_b, increases from -0.027 |e| in the cubic phase to $+0.214$ |e| in the tetragonal phase. Examining separately the σ and π contributions to q_b in the tungstyl group, we note that they both correspond to an increase in covalence in the tetragonal structure with respect to the cubic structure: q_b^σ increases by 0.12 |e|, and q_b^π by 0.13 |e|. This result is in disagreement with ref 6, where the authors found that the deformation is favored by the π interaction, but opposed by the σ interaction. The discrepancy between our results and those of the previous work may be due to the contributions neglected in the extended Hückel method: the mixing of AOs in the full Hamiltonian is in fact far more complicated than that described in ref 6.

It is difficult to attribute a bond order between tungsten and oxygen on the basis of the Mulliken bond population values alone; a comparison of the present results with other solids

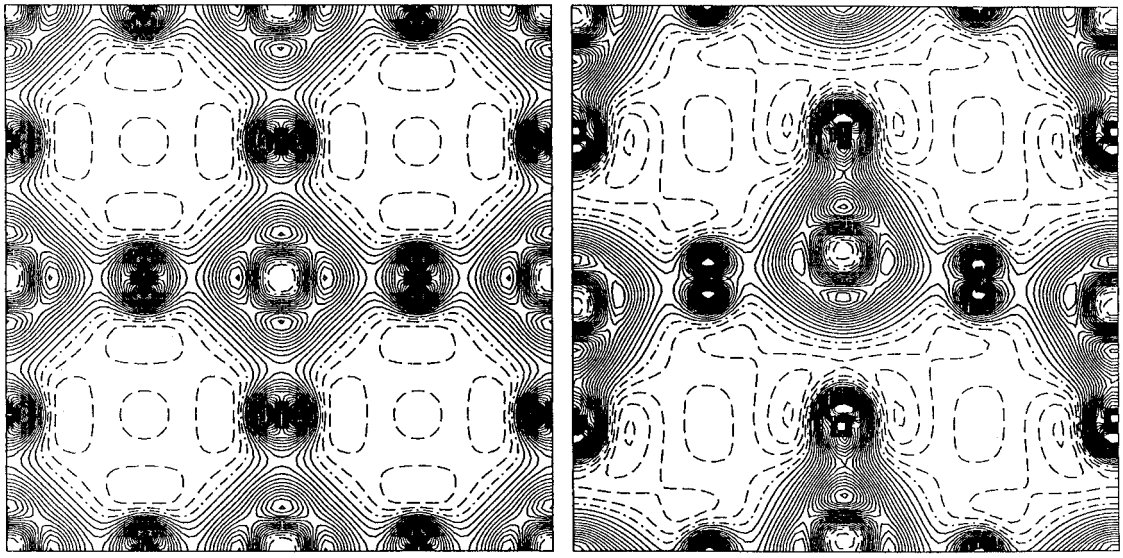

Figure 3. Difference electron density maps (solid minus isolated ions) for cubic (left plot) and tetragonal (right plot) WO_3. Continuous, dashed, and dotted−dashed lines correspond to positive, negative, and zero difference, respectively. The interval between isodensity lines is 0.005 au (electrons/bohr^3). The same basis set has been used in both cases. The map is drawn in the same plane as Figure 1C.

where the structure is better resolved can help our understanding. Because of short-range (exchange) repulsions, in a strongly ionic solid, like MgO or LiF, q_b assumes slightly negative values, typically on the order of -0.05 |e|. The same situation occurs in cubic WO_3 and in other transition metal oxides, like ZrO_2.[30] In quartz, the standard description is that of a single covalent bond between silicon and oxygen; in previous studies performed with the same model and the same Hamiltonian, it was found that q_b ranges between 0.198 and 0.250 |e| according to the basis set employed.[24,31] As a model of a double bond we can consider the vanadyl group in vanadia, V_2O_5. In a recent study performed with CRYSTAL[32] the bond population in the vanadyl group was found to be $+0.359$ |e|. The comparison with these previous results seems then to suggest that a single bond between metal and oxygen is present in tetragonal WO_3.

A final comment can be made on the interaction between second nearest oxygens, which are in close contact. In the earlier study on zirconia[30] and in a similar one on the perovskite $MgSiO_3$,[25] it was found that the symmetry reduction was driven by the decreased repulsion between oxygens in the low symmetry phases. In the present case, the perovskite structure exhibits regions of very low electron density (as can be seen in the map of Figure 3) which might be effectively employed by the oxygens to minimize the O−O repulsion. In cubic WO_3 the distance between all oxygen pairs is 2.66 Å; the tetragonal deformation resolves the degeneracy: because of the elongation along the *c* axis, the distance between axial and equatorial oxygens increases to 2.75 Å; the compression in the equatorial plane causes a decrease in the distance between equatorial oxygens to 2.64 Å instead. When we take into account the multiplicity of oxygen−oxygen pairs in each coordination octahedron, the average distance does not change significantly in the two phases. This geometrical result is reflected in the bond population. The driving force for the symmetry lowering in WO_3 must therefore be attributed to the change in the metal−oxygen interaction, rather than in the oxygen−oxygen interaction.

c. Band Structure and Projected Density of States. We now examine band structures and projected densities of states (PDOS) for the two phases under investigation. These quantities are reported in Figures 4 and 5, respectively.

The pronounced difference in the bonding between cubic and tetragonal WO_3, which emerged from the analysis of the electronic distribution, results in only minor differences in the band structure (Figure 4). The most important is the "nature" of the gap: in both phases the lowest energy state in the conduction band is located at the origin of the Brillouin zone (Γ point); in the cubic phase the highest state in the valence band is located at the M point, while in the tetragonal structure this state corresponds again to the Γ point. The minimum energy excitation corresponds therefore to an indirect transition, M−Γ, for cubic WO_3, and to a direct transition in the Γ point for tetragonal WO_3.

The HF value of the band gap is 0.28 hartree (7.7 eV) in the cubic phase, and is little changed to 0.30 hartree (8.1 eV) in the tetragonal phase. We are not aware of any experimental value reported in the literature. Experience gained in previous studies with HF Hamiltonians suggests that the band gap is systematically overestimated, often by a factor of 2 or more.[33] The values reported are to be considered as an upper limit; they are comparable with the value of 6.0 eV obtained in similar computational conditions for a typical semiconductor like silicon.[33] This comparison would suggest that both cubic and tetragonal tungsten trioxides will be semiconductors.

Together with the total PDOS, in Figure 5 (left) we show the contributions due to single atoms and to the valence d orbitals of tungsten. The contribution to the valence band is highlighted in Figure 5 (right). In each part of the plot, the upper figure corresponds to tetragonal WO_3, the lower part to the corresponding quantity in the cubic phase. We note at this point that because the choice of the zero electrostatic potential in a three-dimensional infinite solid is arbitrary,[34] the position of levels in the two phases is shifted arbitrarily. In the following discussion, therefore, we compare the relative position of levels within the same phase, but we do not compare the absolute energy of corresponding levels in the two different phases. As expected in a highly ionic system, the valence band has a dominant contribution from the anion, while the conduction band

(31) Dovesi, R.; Pisani, C.; Roetti, C.; Silvi, B. *J. Chem. Phys.* **1987**, *86*, 6967.
(32) Kempf, J. Y.; Silvi, B.; Dietrich, A.; Catlow, C. R. A.; Maigret, B. *Chem. Mater.* **1993**, *5*, 641.
(33) Orlando, R.; Dovesi, R.; Roetti, C.; Saunders, V. R. *J. Phys.: Condens. Matter* **1990**, *2*, 7769.
(34) Saunders, V. R.; Freyria-Fava, C.; Dovesi, R.; Salasco, L.; Roetti, C. *Mol. Phys.* **1992**, *77*, 629.

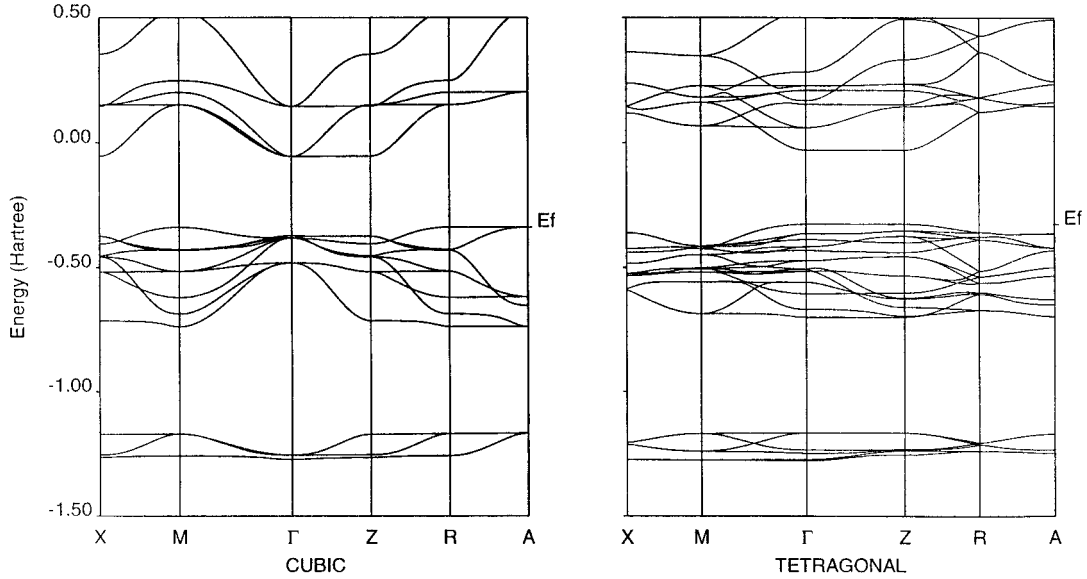

Figure 4. Band structure for cubic (left plot) and tetragonal (right plot) WO_3. For an easier comparison, the band structure of cubic WO_3 is plotted with reference to the tetragonal cell.

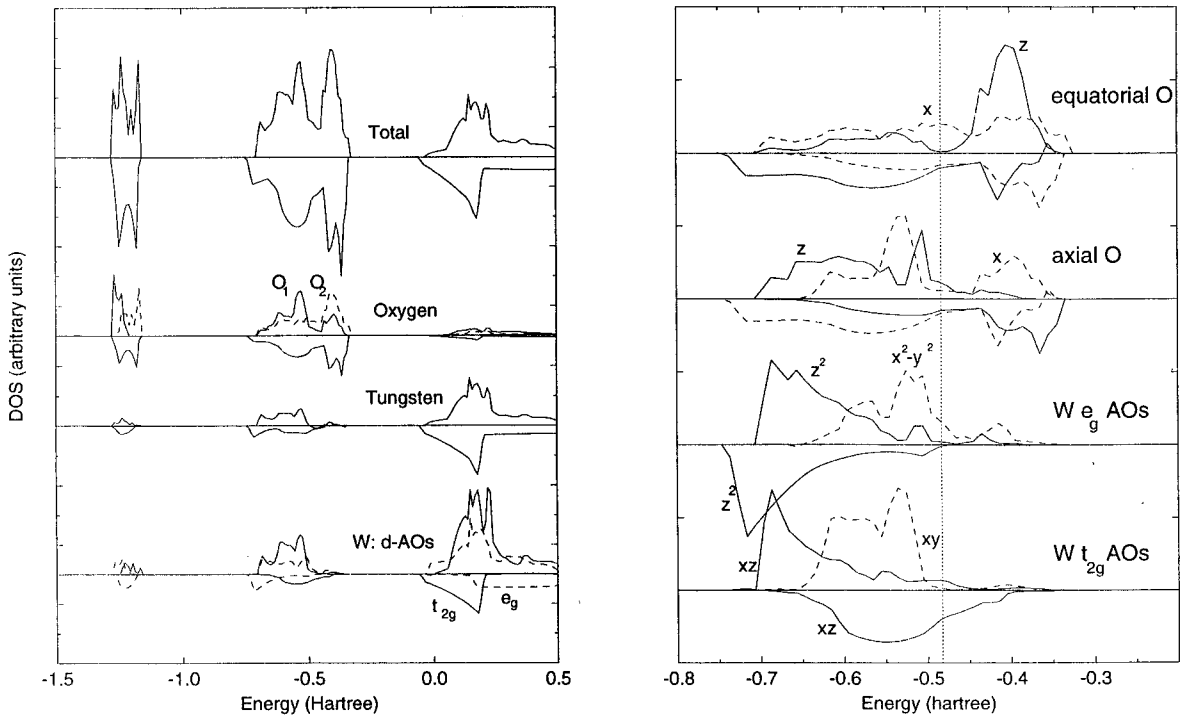

Figure 5. Projected density of states (in arbitrary units) at the HF equilibrium geometry for cubic and tetragonal WO_3. The first plot reports the total PDOS for the solid and contributions from each symmetry unique atom. e_g and t_{2g} d AOs on tungsten are also shown separately. The second plot highlights contributions from single AOs in the valence band. The contribution from the tungsten AOs has been multiplied by a factor of 4 to make it comparable to the oxygens and make the changes more evident. In each diagram, the upper part is relative to the tetragonal phase; the lower part shows the corresponding quantity in the cubic phase.

has a higher contribution from the cation; nonetheless, mixing of tungsten and oxygen AOs both in the valence and in the conduction bands is appreciable, as already suggested by the nonzero population of the d AOs on the metal center.

The position of the tungsten e_g and t_{2g} levels in the band structure deserves some attention. In the cubic phase, on the basis of a simple electrostatic model of a transition metal ion in a octahedral field, one would expect the energy of the triply degenerate t_{2g} level to be lower, relatively to the doubly degenerate e_g level. This is indeed the case for the conduction band, where the component due to the metal d AOs is maximum, but the situation is reversed in the valence band. The back-donation effect already mentioned causes a minor mixing of metal and oxygen AOs; the interaction is most effective for those metal AOs pointing directly toward the nearest neighbor oxygens, that is, for the two e_g levels. This is why these levels in the valence band appear at lower energy than the corresponding t_{2g} level.

Let us now move to the tetragonal phase, and follow the changes occurring in the relative position of valence levels. Four major effects are evident.

(1) The contributions corresponding to the two inequivalent oxygens are clearly resolved. In particular the peak due to the covalently-bound, axial oxygen O_1 lies at lower energy than that of the ionically-bound, equatorial oxygen O_2. We can distinguish two reasons for this result. The first is electro-

static: the axial oxygen is now considerably closer than the equatorial oxygen to the positive charge of tungsten. The magnitude of this effect can be quantified by comparing the relative position in the baricenter of the oxygen 2s bands (in the region of −1.2 hartrees in Figure 5 (left)). The second effect is the increased covalence in the tungstyl group. The sharp peak in the valence band due to O_1 has an important contribution from the oxygen p_z AO (Figure 5 (right)), the one pointing toward the nearest W, and therefore involved in the σ covalent bond formation. This second effect overlaps with the first, and increases the splitting of peaks in the valence band.

(2) The valence band of tetragonal WO_3 (Figure 5 (left)) appears to be split into two sub-bands: one at lower energy (in the region from −0.7 to −0.5 hartree in Figure 5 (right)), with contributions from the axial oxygens and the tungsten ions, and one at higher energies, mostly due to the equatorial oxygens, and with almost zero contribution from tungsten. The separation between the two sub-bands is marked by a vertical dotted line in Figure 5 (right).

(3) The peaks in tetragonal WO_3 are better resolved than in cubic WO_3, an effect that can be attributed to a greater localization of electrons in the former phase; the same effect can be observed in the density maps of Figure 3. Although the perovskite structure has empty spaces of similar dimensions in both phases, only the oxygens in the tetragonal phase exploited these to orient their unshared electron pairs.

(4) The splitting of levels occurring on the metal site (Figure 5 (right)) can be explained in light of the discussion in the previous section concerning the geometric modifications. The relaxation of oxygens that accompanies the displacement of tungsten off-center, causes a decrease of the lattice parameter in the equatorial (*xy*) plane. The two d AOs on tungsten that lie on this plane (the d_{xy} and $d_{x^2-y^2}$) are correspondingly destabilized. On the other hand, the tetragonal phase results in elongation along the crystallographic *c* axis, and the d AOs with contribution in the *z* direction suffer a reduced short-range repulsion from the electrons on oxygens, with a corresponding reduction in their energy.

IV. Effect of Pressure on the Structures

The results of the calculations presented so far refer to the equilibrium geometry at zero pressure (*p*). It would be useful to extend the analysis to the range of experimentally accessible pressure, so as to evaluate the corresponding effect on the crystalline behavior. For instance it has been shown that ReO_3, which has a structure very similar to WO_3, undergoes several pressure-induced phase transformations,[35,36] and it would be useful to see whether WO_3 also shows the same behavior. As would seem reasonable in light of the analysis of the chemical bonding in the crystal performed in the previous section, the covalent component of the tetragonal phase should make it more rigid with respect to the cubic phase, and pressure could provide the driving force for the stabilization of the cubic phase.

The passage from the $E = E(V)$ curve given in Figure 2C to the $E = E(p)$ relation can be effected by means of thermodynamic relations. No thermal effect is taken into account in the calculations, and results are expressed at the athermal limit ($T = 0$ K); in this way we can only focus on phase transitions driven by pressure and on isothermal equations of state. The experimental observable that describes the dependence of the structure on pressure is the isothermal bulk modulus (*B*) (or its inverse, the isothermal compressibility χ). The value of *B* can then be obtained by fitting the $E = E(V)$ curve of Figure 2C.

Different equations of state proposed in the literature[37−43] have been used in the present case to estimate the bulk modulus, and they all agree within 1%; the values of *B* obtained for cubic and tetragonal WO_3 are reported in the last row of Table 3. In contrast to the behavior which might be expected, we see that the bulk modulus for tetragonal WO_3 is lower than its value in cubic WO_3. The latter is therefore stiffer than the tetragonal phase, and on increasing the applied pressure the difference in thermodynamic stability between the two phases increases. This result clearly shows that, for WO_3, pressure does not play a role in changing the chemical structure of the solid. The unexpected pressure dependence of the material deserves a more detailed examination. Let us consider the data reported in Table 4; they represent the change in the unit cell geometry as a function of *V*. This change is directly correlated with the pressure applied to the sample. For each value of V/V_o reported, the internal geometry of the system has been completely optimized, both at the HF level and with correlation. What then is the effect of pressure on the structure of tetragonal WO_3? First of all we see that by increasing *p* (decreasing *V*) the tetragonal deformation *d* tends to the cubic value $\sqrt{2}$, but it requires very high applied pressures (the value $V/V_o = 0.96$ corresponds to an applied pressure of 5.5 GPa, 5.5×10^4 atm.); moreover, on decreasing *V*, z_W increases, and even if the oxygen octahedron were regular, the structure obtained would still be tetragonal. Further revealing information is obtained by examining the bond distances, also reported in Table 4. The 10% change in volume examined causes in fact completely different changes in the three nonequivalent tungsten−oxygen bond lengths. The covalent bond in the tungstyl group (r_1) is left largely unchanged; the distance of the four equatorial oxygens (r_2) is more sensitive to pressure, but the parameter that is most dramatically affected by the change of volume is the longest distance, r_1'. In the range examined the latter changes by 0.15 Å.

In the tetragonal structure, tungsten and oxygen atoms form zigzag planes, and r_1' represents the distance between adjacent planes (this is indicated with the dotted line in Figure 1B). On applying an external pressure on the sample, most of the change induced in the solid is absorbed by the change in the interplanar distance (dotted line in the figure). This is a "soft" degree of freedom, and the bulk modulus of tetragonal WO_3 is consequently lower.

It is also interesting to note the positive change of r_1 that accompanies the compression of the solid. This fact can be explained considering the balance of Coulomb forces acting on the axial oxygen, O_1: the considerable decrease of r_1' that accompanies the compression of the solid brings O_1 to a position that is much closer to the second tungsten ion, to whose charge it is much more attracted. This causes a lengthening of its covalent bond length r_1.

Via the above analysis we can attribute to WO_3 a previously unexpected "layered" behavior, with the layers oriented perpendicular to the crystallographic (001) direction. This property of WO_3 is very similar to the chemical and structural properties

(35) Alkire, R. W.; Larson, A. C.; Vergamini, P. J.; Morosin, B. *Acta Crystallogr., A* **1984**, *40*, C375.
(36) Jorgensen, J. E.; Jorgensen, J. D.; Batlagg, B.; Remeika, J. P.; Axe, J. D. *Phys. Rev. B* **1986**, *33*, 4793.
(37) Murnaghan, F. D. *Proc. Natl. Acad. Sci. U.S.A.* **1944**, *30*, 244.
(38) Birch, F. *J. Geophys. Res.* **1978**, *83*, 1257.
(39) Davis, L. A.; Gordon, R. B. *J. Chem. Phys.* **1967**, 2250.
(40) Bardeen, J. *J. Chem. Phys.* **1938**, *6*, 372.
(41) Slater, J. C. *Introduction to Chemical Physics*; McGraw-Hill: New York, 1939.
(42) Vinet, P.; Ferrante, J. H.; Rose, J. H.; Smith, J. R. *J. Geophys. Res.* **1987**, *92*, 9319.
(43) Brennan, B. J.; Stacey, F. D. *J. Geophys. Res.* **1979**, *84*, 5535.

shown by V_2O_5.[32] Experimental studies of the pressure dependence of tetragonal WO_3 would clearly be of considerable interest.

V. Conclusions

The results obtained for WO_3 presented in this work are consistent with the available experimental data. The present investigation has shed light on the chemical structure of the solid. In particular we have found that, due to its high instability with respect to lower symmetry phases, cubic WO_3 is unstable, and even an increase in pressure cannot force the tungsten ion on-center in its coordination polyhedron. The driving force toward the symmetry breaking is attibuted to the change in the metal−oxygen interaction rather than to effects confined to the metal center alone or to the oxygen−oxygen interaction. Tungsten displaces considerably off-center in its coordination octahedron, and approaches one of the six nearest oxygens. The displacement is stabilized by an increase in covalence between the tungsten and oxygen atoms; they form a rigid unit that is not perturbed by changes, even dramatic ones, occurring in the surrounding crystal. We refer to this unit as a tungstyl group. The increase in covalence in the tungstyl group involves orbitals of both σ and π symmetry along the W−O bond. Finally, the antiferroelectric displacements of the W ions in tetragonal WO_3 form a layered structure in the solid, with the layers oriented perpendicular to the crystallographic (001) direction. It would be desirable to extend the present study to lower symmetry phases, but the computational demands of such a study would be considerable. The present study, however, highlights the contribution that can be made by periodic boundary condition Hartree−Fock techniques to our understanding of structure and bonding in complex transition metal oxides.

Acknowledgment. F.C. acknowledges financial support from EPSRC, Molecular Simulations Inc. (MSI), and ICI Katalco. A.P. thanks the Defence Research Agency for funding.

JA961514U